## Applied and Environmental Microbiology



Environmental Microbiology | Full-Length Text

## Long-duration environmental biosensing by recording analyte detection in DNA using recombinase memory

Prashant Bharadwaj Kalvapalle, <sup>1</sup> Swetha Sridhar, <sup>1</sup> Jonathan J. Silberg, <sup>2,3,4</sup> Lauren B. Stadler<sup>5</sup>

**AUTHOR AFFILIATIONS** See affiliation list on p. 16.

ABSTRACT Microbial biosensors that convert environmental information into real-time visual outputs are limited in their sensing abilities in complex environments, such as soil and wastewater, due to optical inaccessibility. Biosensors that could record transient exposure to analytes within a large time window for later retrieval represent a promising approach to solve the accessibility problem. Here, we test the performance of recombinase-memory biosensors that sense a sugar (arabinose) and a microbial communication molecule (3-oxo-C12-L-homoserine lactone) over 8 days (~70 generations) following analyte exposure. These biosensors sense the analyte and trigger the expression of a recombinase enzyme which flips a segment of DNA, creating a genetic memory, and initiates fluorescent protein expression. The initial designs failed over time due to unintended DNA flipping in the absence of the analyte and loss of the flipped state after exposure to the analyte. Biosensor performance was improved by decreasing recombinase expression, removing the fluorescent protein output, and using quantitative PCR to read out stored information. Application of memory biosensors in wastewater isolates achieved memory of analyte exposure in an uncharacterized Pseudomonas isolate. By returning these engineered isolates to their native environments, recombinase-memory systems are expected to enable longer duration and in situ investigation of microbial signaling, cross-feeding, community shifts, and gene transfer beyond the reach of traditional environmental biosensors.

**IMPORTANCE** Microbes mediate ecological processes over timescales that can far exceed the half-lives of transient metabolites and signals that drive their collective behaviors. We investigated strategies for engineering microbes to stably record their transient exposure to a chemical over many generations through DNA rearrangements. We identify genetic architectures that improve memory biosensor performance and characterize these in wastewater isolates. Memory biosensors are expected to be useful for monitoring cell-cell signals in biofilms, detecting transient exposure to chemical pollutants, and observing microbial cross-feeding through short-lived metabolites within cryptic methane, nitrogen, and sulfur cycling processes. They will also enable *in situ* studies of microbial responses to ephemeral environmental changes, or other ecological processes that are currently challenging to monitor non-destructively using real-time biosensors and analytical instruments.

**KEYWORDS** biosensor, integrase, genetic memory, quorum sensing, recombinase, wastewater, synthetic biology

B acteria continuously sense and respond to dynamic changes in their environment using cytosolic and extracellular sensing systems (1–3). Engineers have leveraged the exquisite sensing capabilities of microorganisms through synthetic biology to program them to sense and report on specific environmental conditions and analytes (4), ranging from the presence of toxic metals (5), organic pollutants (6), and antibiotics (7)

**Editor** Knut Rudi, Norwegian University of Life Sciences, Ås, Norway

Address correspondence to Lauren B. Stadler, lauren.stadler@rice.edu, or Jonathan J. Silberg, joff@rice.edu.

The authors declare no conflict of interest.

See the funding table on p. 16.

Received 13 January 2024 Accepted 20 February 2024 Published 29 March 2024

Copyright © 2024 American Society for Microbiology. All Rights Reserved.

Downloaded from https://journals.asm.org/journal/aem on 17 February 2025 by 98.200.228.83

to essential nutrients (8) and microbial communication signals (9). With most biosensors, reporting is achieved by coupling the sensing of a specific environmental chemical to the production of a visual output, such as enzymes that produce colored products (10, 11), luminescent enzymes (12, 13), and fluorescent proteins (14). Biosensors with visual outputs have enabled rapid detection of analytes within drinking water, serum, and milk with minimal pre-processing (6), and from more complex samples after destructive chemical extraction (15–17). Strategies have been developed to extend visual-reporting biosensors for time-resolved, *in situ* studies within hard-to-image materials by creating custom lab environments such as soil microcosms or rhizotrons with windows that allow continuous imaging of live microbes on the soil surface (9, 18). However, visual reporters have limited use for continuous monitoring in opaque and inaccessible environments (12), limiting their applications in soil, wastewater, and sediment. Biosensors that record information in DNA represent an emerging technology with the potential for environmental sensing in turbid and hard-to-access environments over timescales relevant to ecological processes (Fig. 1A).

Microbes have been engineered to record information about sensed analytes in their DNA using a wide range of enzymes, such as recombinases (19, 20), CRISPR nucleases (clustered regularly interspaced short palindromic repeats) (21, 22), CRISPR integrases (23–25), and polymerases (26, 27). Microbes have also been engineered to record information about uptake of mobile DNA in their 16S ribosomal RNA using ribozymes (28). Among these two biological information storage approaches, information coded in DNA is more stable because the modified nucleic acid is inherited in daughter cells as the programmed cells divide. Thus, it can be retrieved following deployments of varying duration. In contrast, RNA memory is less permanent as the RNA information is degraded within cells. While DNA memory is appealing to use for environmental biosensing, because it records information about historic exposure to analytes (29), it has only been applied in a small number of environmental microbes and materials.

Recombinase-memory biosensors represent one of the earliest innovations of synthetic cellular recording (19, 20). With these DNA memory devices, the conditional expression of a recombinase is used to catalyze the flipping of a DNA sequence flanked by two recognition sites (30, 31). The simplicity of these systems have made them appealing for environmental applications (Fig. 1B), because they only require low-level expression of a single enzyme and short ~40-70 bp recognition sites within the DNA substrate for this enzyme (31, 32); no other host-derived biomolecules are needed. Recombinase memory was first applied in Vibrio cholerae within the mouse gut to sense iron limitation (19). Upon sensing the analyte, the recombinase activated an antibiotic resistance gene, which was detected in various regions of the intestine after sacrificing the mouse and selecting for antibiotic-resistant microbes (19). Recombinase memory has also been used to identify virulence genes in pathogens (33-35), to identify symbiosisactivated genes in Sinorhizobium meliloti (20), to quantify root exudates (36) and contaminants (37) in soils, and to mark specific cell populations in embryos for tracing their lineage to organ formation (38, 39). Although recombinase studies have achieved biosensing within different hard-to-image environments, they have largely involved short, 2-day growth periods. Currently, it remains unclear if existing recombinasememory designs can be used for week-long biosensing applications, or if they must be optimized for sensing in longer deployments.

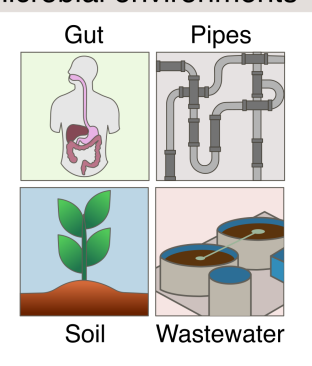
To better understand how to create memory sensors that record and retain binary information about analyte exposure for up to a week following transient exposure (Fig. 1C), we built two recombinase-memory biosensors that write information in DNA about exposure to the sugar arabinose and to the signal 3-oxo-C12-homoserine lactone (C12-AHL), a quorum-sensing molecule used in microbial communication. In environments such as wastewater, quorum sensing regulates many processes, including biofilm formation (40, 41), flocculation (42), and pollutant biotransformation (43), which are important to wastewater treatment performance and process management (42). We investigated the fidelity of this recombinase memory when DNA flipping was used to

### A) Motivation: Inaccessible environments

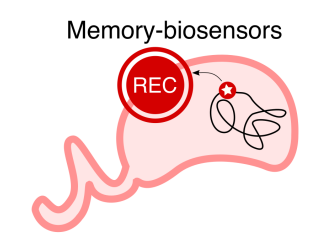
### Transient/rare inputs

## CO Elemental cycle intermediates [C4 to C14]-AHLs Quorum Sensing

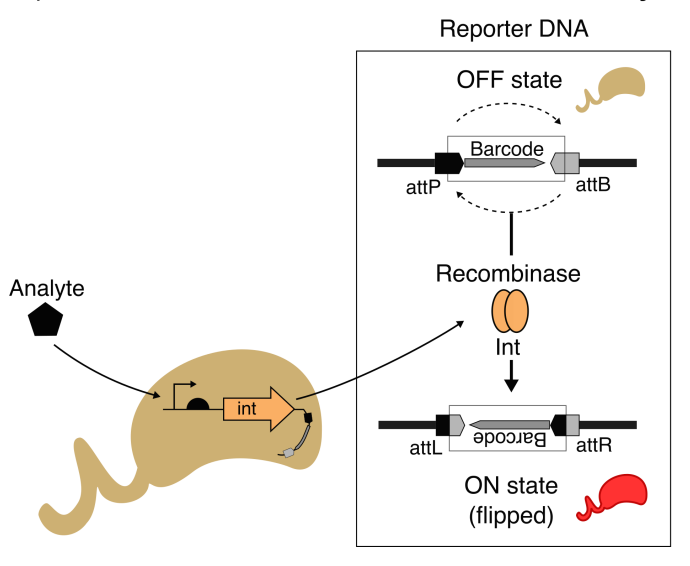
## Inaccessible and opaque microbial environments



### Permanent outputs



### B) Mechanism of recombinase memory



### C) Proof of concept of memory

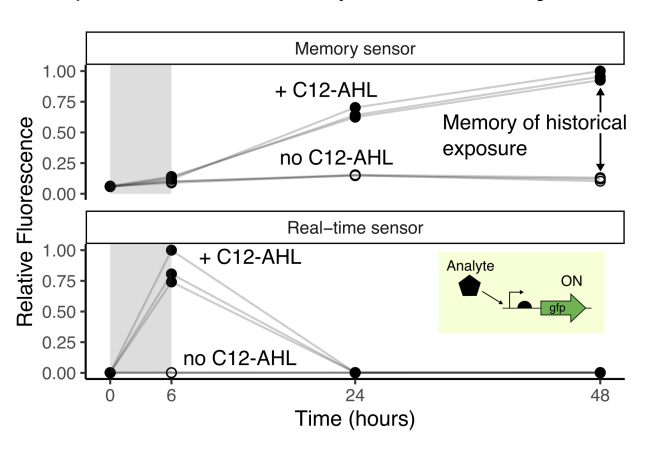


FIG 1 Recombinase memory stores information of historical analyte exposure. (A) Memory biosensors can be deployed into inaccessible, hard-to-image environments for undisturbed monitoring of ecological processes by coupling the detection of transient and rare chemical inputs into permanent DNA modifications. (B) A recombinase-memory biosensor works by conditionally expressing a recombinase enzyme when it senses an analyte. The recombinase binds the DNA attachment sites *attP and attB* and reverses the DNA segment flanked by the sites, thereby encoding information as a genetic memory in the DNA. (C) A memory sensor provides information on historical exposures to environmental chemicals (top), in contrast to a real-time reporter which only provides information during chemical exposure (bottom). Data are shown for reporters of the quorum-sensing molecule, 3-oxo-C12-L-homoserine lactone (C12-AHL). Sensor outputs were measured indirectly by monitoring cellular fluorescence arising from DNA flipping. Three independent cultures of both sensors were exposed to 1 μM C12-AHL for 6 hours in the exponential phase (gray), prior to washing and subculturing for two passages. While the memory sensor retained the fluorescence after the analyte was removed, the real-time sensor's output was not significantly different from baseline at 48 hours (paired sample two-tailed *t*-test, *P* = 0.84). This loss of signal was expected with the real-time sensor, since this biosensor only synthesizes the fluorescent protein in the presence of the analyte. After analyte removal, the fluorescent protein reporter is subject to degradation and dilution as cells grow.

switch on production of a protein reporter and characterized the challenges associated with memory stability. We find that memory declines dramatically within 2 days following analyte exposure when it is coupled to production of a protein reporter. We show that removing the burden of protein expression from the memory system enabled it to function stably for up to 8 days. We further evaluated the application of our memory system in wastewater isolates and the readout of the stored information using quantitative PCR (qPCR). This work paves the way for the application of memory biosensors in wastewater for monitoring fundamental biological processes *in situ*, such as the signals

that trigger biofilm formation, and transient toxic chemicals that are a threat to public health.

### **RESULTS**

### Recombinase memory records analog information

The basic unit of recombinase memory is a segment of DNA that can code binary information: OFF or ON state. In a population of bacteria, multiple digital recordings within each bacterium can result in an analog record of the analyte concentration exposure. Each bacterium contains multiple copies of the plasmid DNA (~5 to 15), and there are billions of bacteria per milliliter of culture. Thus, the quantification of memory depends on the fraction of the cells within the population and fraction of plasmids in each cell having DNA in the ON state. Figure 2A illustrates how transient exposure to small analyte concentrations is expected to only flip a small fraction of the bacteria within the population, while higher concentrations flip an increasingly larger fraction of bacteria into the ON state, until the whole population is converted to the ON state.

To evaluate recombinase memory as an analog sensor for environmental applications, we characterized the performance of a previously described recombinase-memory biosensor for the sugar arabinose (44), and we built another sensor for the microbial communication molecule C12-AHL. We characterized several memory-biosensor properties in *Escherichia coli*, including (i) the stability of the OFF state in the absence of the analyte, (ii) the sensitivity to input analyte concentration; (iii) the dynamic range of the memory signal following analyte exposure, (iv) the stability of the ON state following recording of analyte detection, and (v) the function of the sensor plasmid across different bacteria. To quantify the sensitivity and the dynamic properties of the biosensors, we exposed each memory biosensor to different concentrations of their respective analytes (arabinose or C12-AHL) and quantified the memory at different times after the exposure.

To compare different approaches for reading out the memory, two methods were used (Fig. 2B). First, an indirect method was used in which the green fluorescent protein (GFP) was turned ON by recombinase activation and monitored using the change in fluorescence of the cell. We also used a more direct method that uses qPCR to quantify the amount of DNA in each state. With the qPCR approach, we detected the ON state of the memory by designing a primer pair that binds outside and inside the flipping region, such that amplification only occurs when the memory is in the ON state and after flipping has occurred.

The arabinose sensor performance was evaluated using fluorescence (Fig. 2C) and qPCR (Fig. 2D) readouts. Figures S1 and S2 show the complete flow cytometry distribution and absolute qPCR quantification data, respectively. With both methods of detection, increasing concentrations of the analyte led to an increased fraction of the population in the ON state. At the highest analyte concentrations, the downward trend is interpreted as arising from both a decreased plasmid copy number and selection against cells with plasmids in the ON state caused by cellular burden of the genetic circuit. We quantified the dynamic range of the memory as the ratio of the signal at the maximum analyte concentration (saturated) to the signal of the no analyte control. We found that both outputs presented a similar dynamic range. A similar characterization was performed with the C12-AHL sensor (Fig. S3). A similar trend was observed, with increasing analyte concentrations initially showing more flipping to the ON state, indicated by higher fluorescence intensity, followed by a downward trend at the highest analyte concentrations. These results show that memory biosensors can record analog information about analyte exposure by flipping different fractions of the DNA in the population into the ON state.

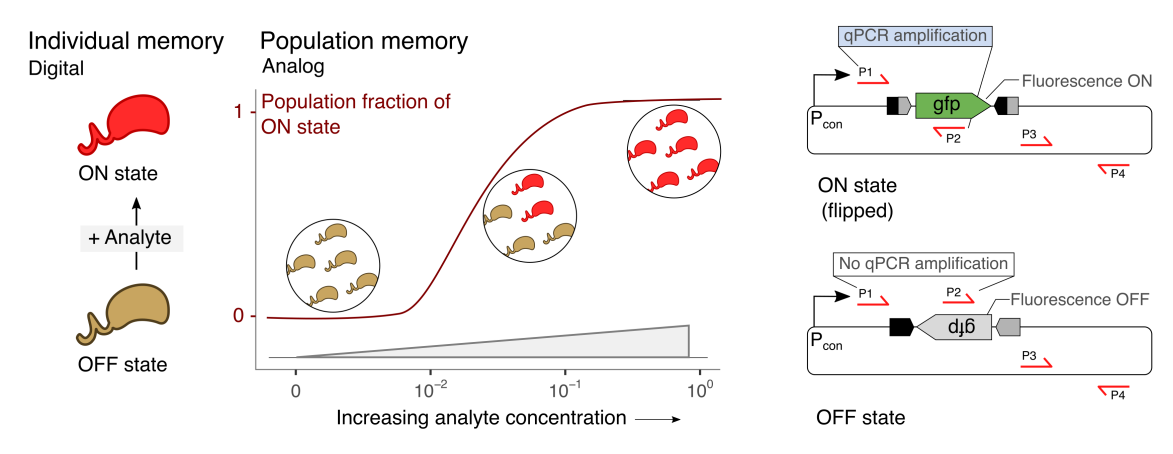
### Memory of analyte exposure is unstable

To assess the stability of the OFF and ON states over time, we grew our initial *E. coli* biosensors in serial batch cultures over 8 days (Fig. 3A). With this protocol, we

exposed the biosensors to analyte at the beginning of the experiment for 1 day, and subsequently passaged them every 24 hours by diluting each stationary phase culture into fresh growth medium lacking analyte. By repeating this protocol for 8 days, we estimate that ~72 generations of growth occurred following analyte exposure. Each day, we quantified the memory signal using single cell fluorescence measurements by flow cytometry and qPCR. With the arabinose sensor (Fig. 3B; Fig. S4A), we observed a signal in the absence of analyte at the beginning of the experiment, which peaked at day 2 and decreased thereafter. When this biosensor was exposed to arabinose, a strong signal was initially observed immediately upon adding the arabinose. However, this signal decreased exponentially, with a half-life of ~1 day for all replicate experiments. After 2 days, the arabinose-induced signal could no longer be differentiated

### A) Individual digital to analog population

### B) Fluorescence & qPCR assay design



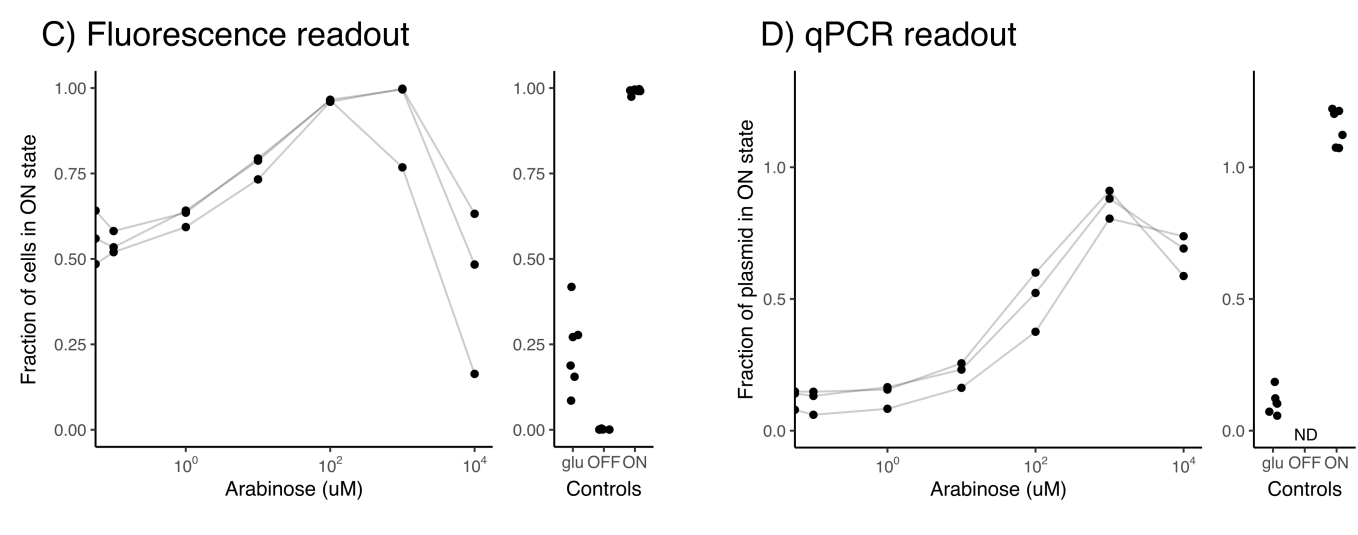


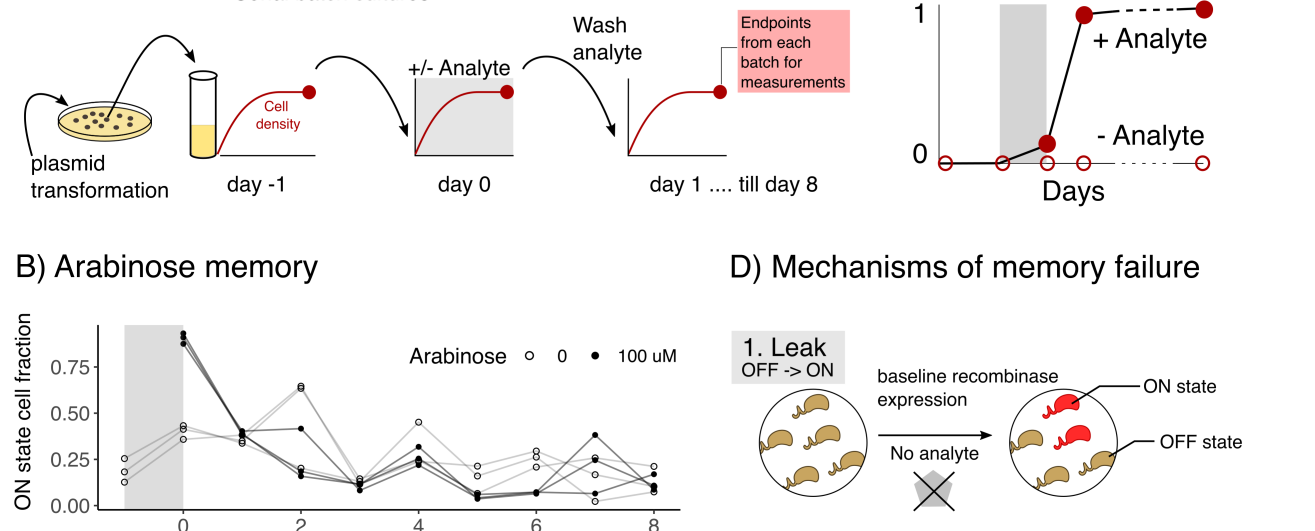
FIG 2 Recombinase memory stores analog information. (A) A digital memory storage device coded within individual bacteria can code analog information at the population level. Exposure of cells in the OFF state (brown) to low analyte concentrations marks a subset of the cells with the memory, switching them to the ON state (red), while higher concentrations increase the fraction of cells in the population to the ON state. (B) Primer sets were designed to read out memory using qPCR. The first primer pair anneals outside the region that is flipped to code a memory (P1) and inside the flipped DNA (P2), such that a product is only formed with the ON state. The second primer set (P3 and P4) was designed to quantify the total reporter plasmid for normalization. (C) The ON state was read out using fluorescence after 24 hours of exposure to a range of concentrations of the input analyte, arabinose. Flow cytometry data from three independent replicate cultures are shown, where the ON state is defined as fluorescence values >99 percentile of the OFF state control. The line connects data from related cultures. (D) The ON state fraction was quantified using qPCR as the copies of flipped state DNA normalized to total copies of the plasmid. Controls are shown in the adjacent sub-panel. The positive control (ON) represents cells harboring the reporter plasmid already in the ON state. The negative controls (OFF and glu) represent cells harboring the OFF state reporter plasmid without the integrase plasmid and the memory biosensor grown with glucose which represses the pBAD promoter. ND, non-detectable signal.

from the background OFF state signal. With the C12-AHL sensor (Fig. 3C; Fig. S4B), we also observed a signal in the absence of the analyte, although this background signal was more stable than observed with the arabinose sensor. With this sensor, the signal following analyte exposure was more stable. The AHL-induced signal remained significantly higher than the OFF state signal until day 6. It decreased by 50% from the maximum value between days 5 and 8 for the different replicate experiments. These results show that both the OFF and ON states of the memory biosensor are unstable over week-long serial cultures, illustrating the limitations of these systems.

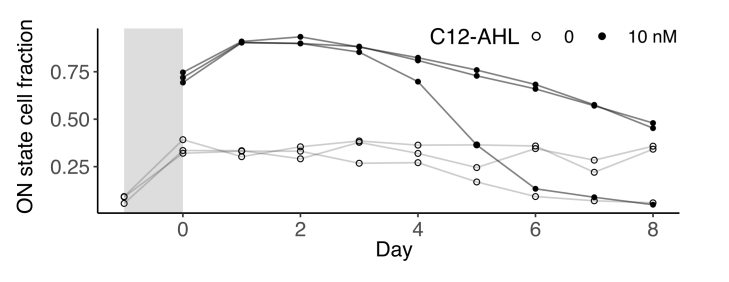
Our findings implicate different mechanisms responsible for the instability of the OFF and ON states (Fig. 3D). The OFF state is thought to be unstable because there is

### A) Memory assay over 9 days

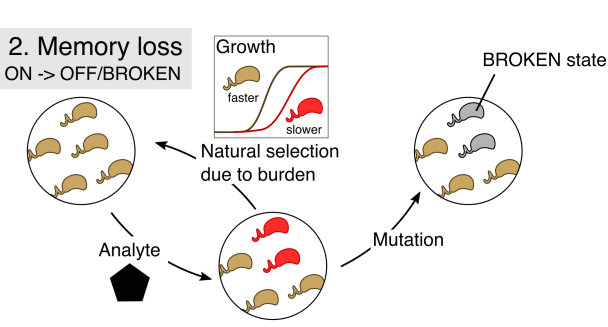
Serial batch cultures



### C) C12-AHL memory



Day



Fraction in ON state

FIG 3 Week-long serial culturing led to memory loss. (A) Experimental design for testing memory stability. Biosensors were grown for ~72 generations using serial batch cultures, with the analyte present only on the first day (shaded region). (B) The arabinose-memory sensor was tested using three independent replicate cultures following 1 day of exposure to 100 µM arabinose (filled circles) or no arabinose (open circles). Samples from the same biological replicates are connected by a line. The fraction of ON state cells expressing GFP were read out by flow cytometry at the end of each day (Fig. S4). The ON state fraction following analyte exposure was unstable and decayed with a half-life of 0.98 ± 0.09 days. Additionally, the ON state fraction remained significantly higher than no arabinose levels only on days 0 and 1 (paired sample one-tailed t-test, P < 0.03). The OFF state was also unstable, as the uninduced cells presented fluorescence. (C) The C12-AHL memory sensor was characterized using 10 nM analyte. Both the ON and OFF states were unstable. However, the memory loss was slower and decayed starting at day 2 with a half-life of 2.8 ± 0.78 days. There was a significant difference between AHL exposed and unexposed samples until day 6 (paired sample one-tailed t-test, P < 0.03). (D) Mechanisms predicted to underlie memory instability. (1) Leaky recombinase expression in the absence of the analyte is predicted to yield a signal in the OFF state (brown). With time, the recombinase accumulates to sufficient levels to flip the memory to ON state (red). (2) The metabolic burden of fluorescent protein expression is predicted to make the ON state unstable. Cells in the ON state are either outcompeted by cells in the OFF state, or they accumulate mutations that abolish fluorescent protein expression resulting in a BROKEN state (gray). Half-lives were obtained by fitting a single exponential, c·e-kt, to the data.

April 2024 Volume 90 Issue 4

sufficient baseline expression of the recombinase in the absence of the analyte to flip some of the DNA. The ON state is thought to be unstable due to the fitness burden that arises when expressing a fluorescent protein, which results in selection pressure favoring faster-growing OFF state cells. Also, the fitness burden was thought to induce mutations that abolished the fluorescence of cells that had been switched to the ON state, termed as BROKEN states. After exposure to analyte, we observed a large deletion of ~1.4 kb in the memory-reporter plasmid on day 8 (Fig. S5), supporting the concept of a BROKEN state. Taken together, our results suggest that long-duration memory systems are challenging to implement due to challenges with both the OFF and ON states.

### Memory is more stable when the protein output is removed

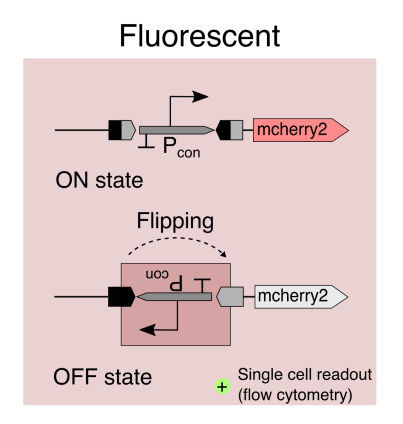
To learn how to improve the stability of the recorded information, we created alternative designs for the memory biosensor. We had three goals with these designs: (i) decrease the baseline recombinase expression, (ii) minimize sequence repeats and remove non-functional intergenic DNA to decrease chances of homologous recombination that lead to the BROKEN state over time, and (iii) consolidate the sensor system into a single mobilizable plasmid with a broad host range origin of replication (pBBR1) to enable its portability into environmental isolates. These experiments were performed using plasmid-encoded genetic circuits to allow for facile testing in multiple strains.

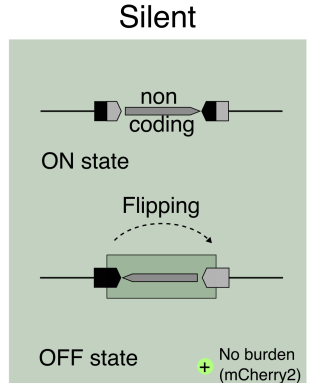
To investigate how decreasing the background recombinase expression affects memory performance, we mutated the recombinase's ribosome binding site (RBS). A library of 56 RBS variants was designed that contained variants predicted to present decreased translation initiation rates (45). Among these, five presented a decrease in the background GFP signal in the absence of analyte (Fig. S6A). These optimized systems presented a ≥10-fold increase in GFP signal upon analyte addition (Fig. S6B), all of which had gains in signal that were greater than the original system tested. When these new designs were used to evaluate the stability of the memory system over 10 days, we found that they uniformly presented a lower background GFP signal (Fig. S7). These designs recorded detection of an analyte like the original design, and they presented transient information storage which rapidly decayed over 2 days. One of the variants was able to record the detection of two sequential pulses of analyte; the parental design could not accomplish this type of information storage. These results demonstrate that decreasing the translation initiation of the recombinase is an effective strategy to decrease the background signal (i.e., improve OFF state stability). However, this change alone did not extend the stability of the stored information due to ON state instability.

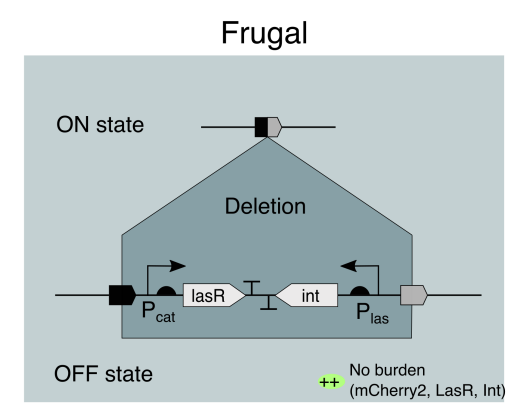
To improve ON state stability, we built three new plasmids that avoided DNA sequence repeats and included only DNA that was critical to biosensor function using a hierarchical golden gate cloning method that combined each functional element, including the promoters, translation initiation sequences, coding sequence of the genes, terminators, an antibiotic selection gene, and a broad host range origin of replication (46). When designing these plasmids, we minimized sequence repeats with the potential to cause mutations that lead to failure of the genetic circuit (47). Figure 4A shows the three different memory designs that were built, which differ in their potential cellular burden on the host. In the first design, called "Fluorescent," the recombinase flips a promoter, thereby turning on the production of a red fluorescent protein, mcherry2. In the second design, called "Silent," the recombinase flips a short, non-coding DNA sequence. In the third design, called "Frugal," the recombinase deletes the LasR analyte sensor and the recombinase, thereby creating a smaller plasmid (6.8 kb to 4.2 kb) that is expected to create a smaller resource burden on cells.

After sequence verifying the plasmids encoding the new designs, we tested their ability to remember exposure to an analyte (C12-AHL) over 8 days using *E. coli* and measured the memory performance by flow cytometry and qPCR. The ON state signal from cells containing the Fluorescent design rapidly decayed over time (Fig. 4B), as observed in the initial designs. In contrast, we found that the ON states of the Silent and Frugal designs were both stable for 8 days following exposure to analyte, presenting

### A) Designs to reduce burden of ON state

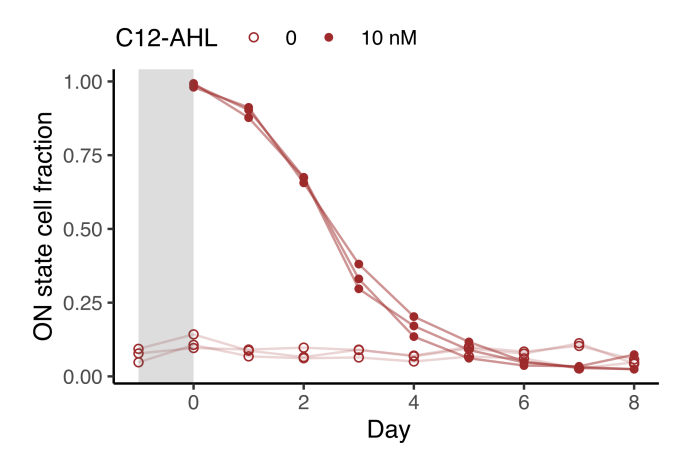






### B) Fluorescent memory is unstable

## C) Burdenless designs are stable



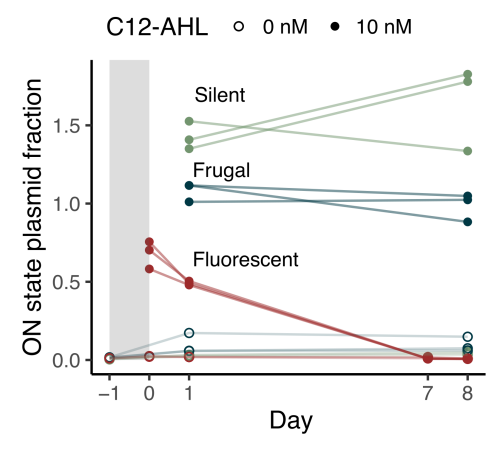


FIG 4 Memory designs can extend the duration of memory utility. (A) The Fluorescent (red), Silent (green), and Frugal (blue) biosensor designs all use a broad host range origin to enable studies in diverse bacterial species, and they lack repeat sequences that can lead to deleterious homologous recombination. Upon sensing the analyte, the Fluorescent design produces fluorescence similar to the parent design, the Silent design flips a non-functional DNA region, and the Frugal design deletes the sensor components (*lasR* and *int* recombinase) to yield a smaller plasmid that is expected to minimize cellular burden. (B) The Fluorescent memory was tested for stability using three independent replicate cultures following a 1 day of exposure to 10 nM C12-AHL (filled circles) or no C12-AHL (open circles). The y-axis shows the fraction of cells in the ON state, gated by fluorescence (Fig. S8), over the duration of the experiment. (C) For each design, the memory output is shown for the same experiment, measured by qPCR. The fraction of the plasmids in the ON state is defined as the copies of flipped state DNA normalized to the total copies of the plasmid; the latter was measured at the start and end of the experiment. To evaluate stability, we assessed whether the signal was significantly different when comparing days 1 and 8 of the experiment (paired sample one-sided t-test on C12-AHL exposed samples, for d1 > d8: Fluorescent: P = 1e - 4, Silent: P = 0.8, Frugal: P = 0.16). The ON state plasmid fraction values that exceed the theoretical maximum of 1 are thought to arise because they were calculated using the absolute copy numbers of two different amplicons, which were quantified using two different standard curves (Fig. S11).

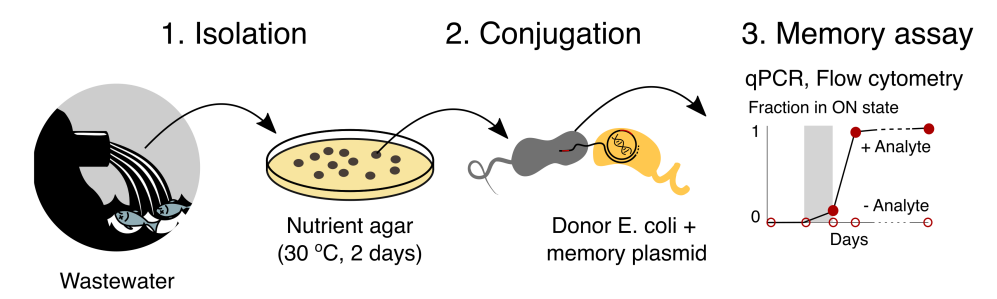
signals on days 1 and 8 that differed by <30% or 0.2-fold (Fig. 4C). Analysis of the fluorescence of individual cells harboring the Fluorescent design revealed low recombinase leak in the absence of analyte (Fig. S8). Taken together, these results show that the Silent and Frugal designs present improved performance. This trend is thought to arise because these designs eliminated the cellular burden of fluorescent protein expression.

### Memory in wastewater environmental isolates

To enable biosensing within wastewater, we tested the optimized memory-biosensor plasmids in bacteria isolated from untreated wastewater. To obtain microbes for this test, influent wastewater was streaked onto nutrient-agar plates, and the antibiotic

sensitivities of the individual isolates was characterized to identify appropriate concentrations for plasmid selections. The memory sensors were then conjugated into each isolate by mating using *E. coli* as a donor strain (Fig. 5A). Once the transformed microbes were obtained on selective plates, we evaluated the ability of three wastewater *Pseudomonas* isolates to stably record exposure to the analyte C12-AHL over 8 days (Fig. S9). For these experiments, we evaluated information stored by the sensors using qPCR. We also compared the performance of one *Pseudomonas* wastewater isolate with *E. coli* with the Fluorescent design. We found that the *Pseudomonas* isolate was more stable in the ON state following exposure to analyte as compared with *E. coli* (Fig. 5B, left panel). With the *Pseudomonas* isolate, the half-life of the information stored was ~4 days, versus ~1 day for *E. coli*. For the Silent design, the signal from the *Pseudomonas* isolate

### A) Engineering wastewater isolates as memory-biosensors



### B) Memory biosensors function in wastewater isolates

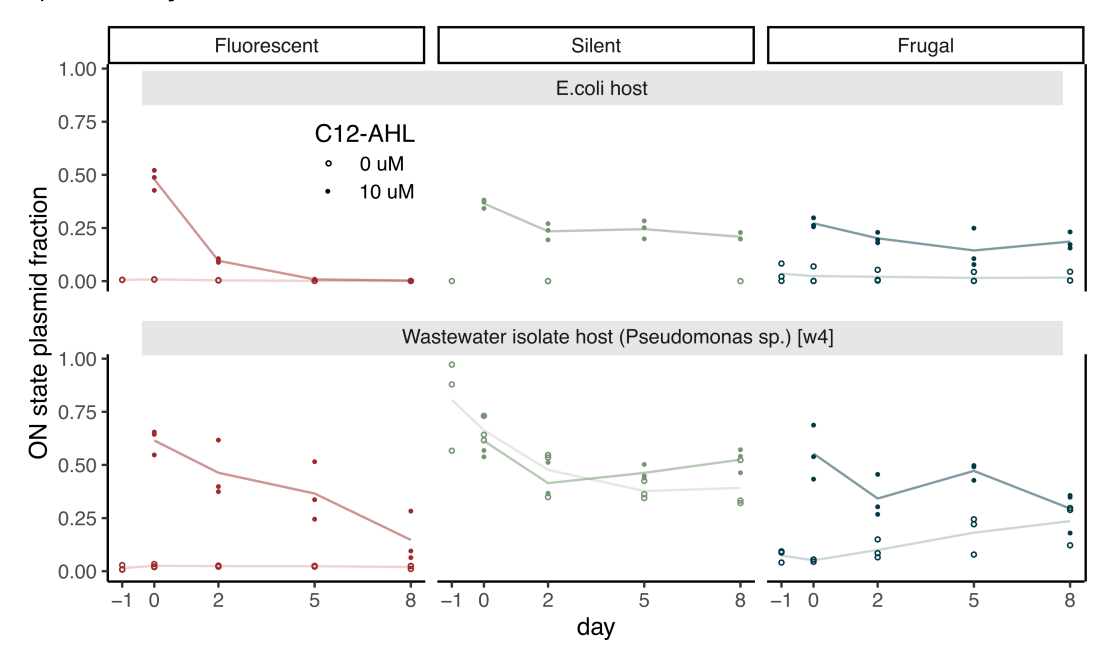


FIG 5 Memory designs function in wastewater microbes. (A) To test memory in wastewater isolates: (1) wastewater was streaked on nutrient agar plates to isolate colonies and characterized using 16S rRNA sequencing (2), the memory-biosensor plasmids were conjugated from *E. coli* donors into the wastewater isolates, and (3) memory performance was characterized using qPCR. (B) A comparison of the memory designs in *E. coli* (top) and one wastewater *Pseudomonas* isolate (bottom). The performance of the Fluorescent (red), Silent (green), and Frugal (blue) designs are compared. For each experiment, we measured the fraction of plasmid in the ON state as in Fig. 4, with data from three independent cultures shown as points, and a line connecting the averages. With the Fluorescent design, analyte exposure yielded a signal that decayed with a half-life of  $1.0 \pm 0.1$  days with *E. coli* and  $3.6 \pm 0.8$  days with the isolate (fit to a single exponential model). With the Silent design, analyte exposure yielded a significantly higher signal than without exposure when pooled across days in *E. coli* (P = 0.74). With the Frugal design, analyte exposure yielded a significantly higher signal than the control on all days with *E. coli* (P = 0.0.04) and with the isolate (P = 0.0.04). All the P-values were obtained using a paired sample one-tailed t-test. Missing points for Silent in *E. coli* indicate that there was no qPCR detection for flipped.

April 2024 Volume 90 | Issue 4 10.1128/aem.02363-23 **9** 

exposed to analyte was similar to cells grown in the absence of analyte (Fig. 5B, middle panel). This suggests that the cells were already in the ON state when the experiment began. This can be contrasted with the *E. coli* biosensor containing this design, which did not present a signal in the absence of analyte. With the Frugal design, the signal in the *Pseudomonas* isolate increased upon addition of analyte (Fig. 5B, right panel). However, this design presented a signal that increased with time in the absence of analyte as well. In contrast, the *E. coli* sensors presented a memory signal that remained higher than the background signal after eight days. These results show that two of our three memory biosensor designs yield a signal within a wastewater *Pseudomonas* isolate without optimization.

We hypothesized that the background signal observed with the Frugal design in the *Pseudomonas* isolate could arise through two mechanisms. The genetic program could express the recombinase in the absence of the analyte, and/or the isolates could synthesize the C12-AHL analyte being sensed. To address the latter possibility, we investigated whether the different wastewater isolates produce C12-AHL by incubating the spent media from cultures of each isolate with an *E. coli* C12-AHL biosensor. With this analysis (Fig. S10), the spent medium from each culture lacked sufficient C12-AHL to activate the *E. coli* fluorescence sensor, which uses the same transcriptional regulator as our memory biosensors for sensing the analyte. This finding suggests that it is more likely that the wastewater isolates with the Frugal and Silent systems present low-level recombinase expression in the absence of analyte. Thus, the regulatory regions which were optimized for *E. coli* expression could be further optimized in the wastewater isolate to improve performance.

### **DISCUSSION**

Our results show that recombinase-memory biosensors can be engineered to record exposure to an environmentally relevant analyte within DNA using both *E. coli* and a wastewater *Pseudomonas* isolate. We use the memory biosensor to detect C12-AHL, a microbial communication molecule that enables coordinated microbial action such as biofilm formation, and flocculation, which are important to wastewater treatment performance and process management (42). The transcription factor that we employed in our genetic circuits to track C12-AHL has been used to detect AHLs *in situ* (48), suggesting that our memory biosensors will have the necessary sensitivity to detect this analyte under some wastewater conditions. We also show how this form of memory for environmental analytes can be programmed to function for up to 8 days. Prior studies using recombinase memory have tested performance over shorter day-long growth (19, 20, 33, 37). Here, we extended the utility of this type of memory to longer timescales by minimizing the cellular burden of the biosensor components and tightly regulating the conditional expression of the recombinase, which writes information in DNA (44).

Our results identify design strategies to improve the stability of recombinase-memory biosensors. First, baseline expression of the recombinase was tuned down by decreasing the strength of translation initiation to minimize false recording in the absence of exposure to the analyte. This tuning, accomplished using a thermodynamic model for translation initiation (45, 49), is especially important in long-duration applications of memory biosensors, as even low-level recombinase expression can lead to production of significant ON state over week-long durations. Another advantage of low recombinase expression is that it avoids the fitness burden on cells when exposed to high concentrations of the analyte, which resulted in lower than expected ON state. Second, streamlined designs that remove intergenic regions and minimize sequence repeats should be created to minimize mutations that can arise from homologous recombination (47). Third, the cellular burden of storing information in cells should be minimized. We evaluated two different approaches to minimize this burden. One approach was to create a Silent design that records information in DNA without expressing a fluorescent reporter. The second was to create a Frugal design that removed the sensing

components themselves in the process of recording. Among these two approaches, the Frugal design performed better within a wastewater isolate. These approaches were successful at improving the longevity of memory biosensors within *E. coli*, and they are expected to be generalizable for optimizing performance in other bacterial hosts.

Further improvements could be explored to minimize the signal in the absence of analyte and improve the stability of the recorded information. Two possible mechanisms that could trigger the background signal that were not explored in this work are (i) the presence of native recombinases in the host organisms that may cause a low level of recording, and (ii) the use of inducible promoter design with inherent baseline activity. For the former, bioinformatic analysis can be used in the future to identify native recombinases in strains targeted for genetic programming, and in vitro and in vivo testing can be used to parse out mechanisms of native recombination that interfere with the stability of synthetic recombinase circuits. For the latter, a non-zero baseline expression of the recombinase is inevitable with the current inducible promoter design due to the kinetics of transcription factor binding (50). This challenge can be overcome by incorporating a secondary control on recombinase expression, such as constitutive expression of an inhibitory antisense RNA that inhibits the translation of the recombinase and imposes a threshold of analyte sensing before recombinase protein is synthesized and recording occurs (50). Another strategy to improve memory biosensors is to integrate them into the chromosome, which would result in a lower copy number and hence a lower baseline expression, along with improved stability. Chromosomal integration would also be the method of choice to make the sensor function within an environmental community as there would be no need for antibiotic addition to maintain the plasmid.

Sensors engineered from environmental isolates are expected to be better equipped to survive in their native environment compared to non-native *E. coli*, which is necessary for long-duration applications (51, 52). This study represents the first time that recombinase-memory sensors have been tested in non-model bacteria, specifically in natural isolates from wastewater. Our findings highlight the opportunities and challenges of using synthetic biology to program memory biosensing in natural isolates. While we demonstrated the application of our optimized memory biosensor in an undomesticated bacteria isolated from wastewater, the isolate did not perform as well as the optimized system in *E. coli*. This finding illustrates how differences in transcriptional and translational regulation across different microbes can lead to variation in the performance of the memory biosensor (53).

Future work will require optimizing memory biosensors in environmental isolates for applications in mixed communities. Our study can guide the workflow for building and deploying memory biosensors in different environments of interest. First, microbes will need to be isolated from the environment of interest and programmed by conjugating memory plasmids into them. The isolates' recording ability and baseline signal will then need to be characterized in pure cultures. For these studies, microbes should be chosen for programming that are consistently found in the environment of interest at a detectable abundance. Second, memory biosensor design should be optimized within the targeted isolate and growth condition of interest using a library of regulatory elements as described here. Such studies can identify architectures (e.g., Frugal) that minimize baseline signal and maximize stability. To allow for facile mixed community experiments, the genetic circuits will then need to be integrated into the chromosome, and biosensor performance will need to be tested in environmental samples of increasing complexity. For wastewater, this may include testing performance within a synthetic microbial community and within an artificial sewage matrix. These mixed community studies should be carried out in chemostat bioreactors to retain microbial diversity and to test the effects of operational parameters such as oxygen, temperature, and dilution rates on biosensor fitness. Finally, the memory biosensors can be deployed into environmental samples within safe custom devices or bioreactors in the laboratory for studies in real communities. When mixed with communities, the memory biosensors

will record binary information about exposure to the analyte, even if that exposure to analyte was transient. The recorded information can then be read out using qPCR after acquiring samples at different time points following introduction into the system.

Memory biosensors are expected to complement -omics methods and time course measurements using real-time biosensors. Microbial communities and their functions can be interrogated using systems-level -omics approaches such as genomics and transcriptomics (54-56), or the targeted detection of particular biomolecules produced by the community using analytical chromatography-based methods (57-59). These methods are limited to providing snapshots of the community at a single point in time, due to their destructive nature during sample processing. When studying microbial communities over time, real-time biosensors present an advance over analytical sensing approaches, since live organisms can be deployed into the community to report on the presence and quantity of particular analytes that are bioavailable to the biosensor over time (13, 60). Given that most real-time biosensors report via visual outputs (9, 61, 62), measuring the biosensor's output requires optical access to the microbes which is not possible in opaque environments such as soil and wastewater. Memory biosensors that record the presence of analytes could be deployed in such scenarios. Recombinase-memory biosensors are expected to record any transient exposures to the analyte throughout the full duration of the incubation, thereby removing the requirement of continuous monitoring. This type of information occurs at the expense of temporal and quantitative information about the analyte. The use of qPCR for reading out the stored information allows for sensitive detection. Given that qPCR is widely used for environmental microbiology (63), this approach for memory biosensor readout is expected to be widely accessible.

In the future, memory biosensors are expected to be useful for reporting on the presence of short-lived metabolites, which are produced intermittently over a longer timescale. For example, microbial cross-feeding involves the exchange of metabolites that are consumed rapidly, thereby making it challenging to directly measure the presence of such cryptic nutrients in the environment. Many intermediates such as nitrite or sulfide are involved in cryptic carbon, nitrogen, and sulfur cycling both within and between microbes, and form critical processes in wastewater treatment systems (64, 65). Memory biosensors should also be useful for studying microbial communication that underlies biofilm formation and flocculation within wastewater that is mediated by quorum-sensing molecules such as AHLs, which could be unstable due to high pH or degradative lactonase enzymes (66–68). By using different orthogonal recombinases (44, 69), wastewater memory biosensors could be created that simultaneously record information about exposure to different types of molecules in the same community.

### **MATERIALS AND METHODS**

### Chemicals

Reagents for growth media, antibiotics, and inducers were purchased from Sigma Aldrich. Enzymes for molecular biology (Bsal-HF v2, T4 DNA ligase, Taq ligase, T5 exonuclease, and Phusion DNA polymerase) were from New England Biolabs, and qPCR master mixes were from PCR Biosystems. Primers were purchased from Sigma Aldrich, and probes were from Integrated DNA Technologies and LGC Biosearch Technologies. DNA extractions were performed using Qiagen Miniprep Kit.

### Isolating wastewater bacteria and conjugation

Untreated wastewater samples stored at 4°C were spread onto YPS agar (4 g/L yeast extract, 2 g/L peptone, 25 g/L sea salts) or Luria broth (LB) agar medium. They were grown at room temperature (~25°C) for 2 days, and colonies with different morphologies were re-streaked before inoculation in super optimal broth with catabolite repression (SOC) (70). The sensitivity of individual isolates to kanamycin and chloramphenicol was

characterized by serial dilution spotting on LB agar plates with different concentrations of the antibiotics. Memory plasmids were transformed into the donor strain, *E. coli* MFDpir by heat shock (71), and this strain was used as a donor for conjugation. Donors and recipients were grown separately to stationary phase at 37°C and room temperature, washed in sterile-filtered phosphate buffered saline (PBS) twice (72), mixed at a 1:1 ratio, spotted onto LB agar medium in a 96-well deep-well block, and incubated for 24 hours at room temperature. Microbial mixtures were resuspended in PBS (500  $\mu$ L), washed, and spotted onto selective medium. Selected colonies were re-streaked on LB agar plates, individual colonies were used to inoculate liquid cultures, and cultures were screened for fluorescence with C12-AHL (10  $\mu$ M).

### **Bacterial growth**

DNA construction and assembly was performed using E. coli DH10B grown in LB medium. Memory experiments were performed in E. coli MG1655, a strain that has been maintained in labs with minimal genetic manipulation (73). For memory experiments, E. coli were grown in M9 minimal medium (M9-glucose) containing 0.4% wt/vol glucose, 0.2% casamino acids, and antibiotics at 37°C (74). Memory experiments in wastewater isolates were performed in LB medium containing 10 g/L NaCl, 10 g/L tryptone, and 5 g/L yeast extract, incubated at 30°C. For all strains, we used 50 µg/mL kanamycin. However, the chloramphenicol concentrations varied by strain: E. coli (34 μg/mL), w4 isolate (100 μg/ mL), and the w17 and w23 isolates (200 µg/mL). For the arabinose titrations, 0.4% glycerol was substituted for glucose in the M9 medium, since glucose represses the pBAD promoter induced by arabinose (75). To induce maximal recombinase expression in E. coli, 100 µM arabinose or 10 nM C12-AHL was included in the growth medium during subculture. For the wastewater biosensors, 10 µM C12-AHL was used for maximal induction. All assays were performed using three independent colonies (biological replicates) grown until stationary phase (~18 to 24 hours) at 37°C in M9-glucose (500 μL) with necessary antibiotics in 96-well deep-well blocks (Analytical Sales and Services, SKU: 59623-23) that were shaking at 650 rpm.

### Plasmid design

All vectors used in this study (Table S1) were constructed using Golden Gate Assembly (46). Vectors for arabinose memory (pAra) and the GFP reporter of recombinase activity (pRec1-OFF) were obtained from Addgene (44). In pAra, the serine recombinase from Staphylococcus haemolyticus (Uniprot: Q4L3S2\_STAHJ) is expressed under the pBAD promoter. The pBAD promoter is induced by arabinose, which binds to the transcriptional activator AraC, expressed constitutively from the same plasmid. In the pRec1-OFF plasmid, a constitutive promoter is situated upstream of the qfp gene, but the gene is inverted in direction with respect to the promoter, so GFP is not expressed. To create the flipped pRec1-ON plasmid as a positive control, E. coli DH10B was transformed with pAra and pRec1-OFF, grown in LB medium with 1 mM arabinose for 16 hours at 37°C, and streaked onto LB agar plates containing chloramphenicol. Individual colonies were used to inoculate LB liquid cultures containing chloramphenicol, the plasmid was extracted from individual colonies, those plasmids were transformed into DH10B to isolate pRec1-ON, and the purified plasmid was sequence verified. pAHL1 contains the same recombinase as pAra, but it is controlled by a synthetic pLas promoter from Pseudomonas aeruginosa (BBa K649000, International Genetically Engineered Machine [IGEM] registry) (76). The pLas promoter is activated by C12-AHL when bound to LasR (BBa\_C0179, IGEM registry), which is expressed constitutively from the same plasmid. The plasmids (pAHL1\_M1 to pAHL1\_M5) with weaker RBS were screened from the RBS library built using Gibson assembly of the amplified pAHL1 backbone without the RBS (77), with a bridging single-stranded DNA oligo containing the RBS library (Table S2). The optimized plasmid designs (pAHL2\_Fluorescent, pAHL2\_Silent, and pAHL2\_Frugal) were assembled using hierarchical Golden Gate Assembly (46) by incorporating double-stranded DNA fragments (Twist Biosciences) containing the att sites of the flipping register

along with the other gene constructs: pCat-catRBS-LasR and pLas-int8. The Fluorescent version included a constitutive promoter (attB-invertible[<J23110 >tVoigtS14]-attP) next to mcherry2, the Silent version included the non-coding sequences (attB-non-coding-attP), and the Frugal version had attB and *inverted*-attP sites flanking the other gene cassettes.

### **DNA** sequencing

Wastewater isolates were cultured in LB30 growth medium (LB with 30 g/L yeast extract) at room temperature for 24 hours. Their genomic DNA was extracted using magnetic bead purification using the RSC PureFood GMO and Authentication Kit (Promega). Whole genome nanopore sequencing was performed by SNPsaurus LLC. Taxonomic analysis was conducted using Mash v2.3-6 (78) against Refseq genomes database (Table S5). In the memory-stability experiment, the pRec1-ON plasmids extracted on days 0 and 8 were sequenced. The consensus sequences were aligned to the original template to establish changes that arose over time, which revealed a 1,398 base pair deletion.

### **Short-duration memory experiments**

Real-time AHL-reporter (76) and memory-reporter plasmids (pAra + pRec1-OFF) were transformed into *E. coli* MG1655. Three independent colonies were inoculated into LB medium, grown until stationary phase, diluted 1:100 into LB containing 1  $\mu$ M C12-AHL, and grown for 6 hours. Subsequently cultures were centrifuged, washed in PBS, and subcultured twice for 18–24 hours each without the C12-AHL. Green fluorescence of all cultures resuspended in PBS at the end of each timepoint was quantified with a plate reader (Tecan Spark, excitation 488 nm, emission 511 nm, gain 140, z-position 20,000  $\mu$ m). Autofluorescence background calculated from MG1655 cells was subtracted, and fluorescence was normalized to optical density (OD<sub>600</sub>) to account for differences in cell growth.

### Recording information by varying arabinose concentrations

Cells co-transformed with the conditional-recombinase (pAra) and the memory-reporter (pRec1-OFF) plasmids were grown on LB agar plates containing glucose and three colonies from each plate were inoculated and grown for 24 hours while shaking at 650 rpm. Cells transformed with memory-reporter plasmids in the OFF (pRec1-OFF) and ON (pRec1-ON) states were also grown as controls. These cultures were then diluted 1:100 into M9 glycerol containing arabinose at different concentrations and grown for 24 hours. Aliquots of the induced cultures were diluted 1:100 in PBS with 0.1% Tween 20 (PBST) and used for flow cytometry. The same cultures were also subjected to qPCR after resuspending in water, performing a 5× dilution, and using heat lysis.

### Flow cytometry analysis of whole cell fluorescence

Cultures in stationary phase from experiments stored at 4°C for 3–9 days were resuspended by pipetting and diluted 1:100 into 500 µL PBST in 96-well deep-well blocks. Samples were run on a spectral flow cytometer with autosampler (Sony SA3800) using the low sample pressure setting. Fluorescence wavelengths were calibrated using *E. coli* MG1655 expressing *gfpmut3*, *mcherry2*, or no fluorescent protein. To calibrate fluorescence, eight-peak beads (Spherotech, RCP-30-5A) were used to establish how fluorescence relates to standardized units of molecules of equivalent fluorophores using FlowCal software (79). Fluorescence data were processed using custom R scripts incorporating flowWorkspace (80), openCyto (81), and ggcyto packages (82). Median values extracted from a pool of three biological replicates were plotted. Code used for processing is available on Github (https://github.com/ppreshant/flow\_cytometry/).

### Lysis and quantitative PCR

Aliquots of M9 cultures (20 µL) were centrifuged, resuspended in water, diluted into 100 µL water in PCR plates, and heated at 95°C for 10 minutes to achieve a quick lysis and high-throughput DNA extraction with small sample volumes (83). For Fig. 5B, cultures in LB (20 µL) were directly diluted into water for lysis without prior resuspension. These dilute microbial lysates were used directly in the qPCR reactions. Dilute lysate (4 µL) was assayed in a 10  $\mu$ L qPCR reaction with qPCRBIO Probe Mix Lo-ROX master mix (PCR Biosystems, PB20.21-01) containing 0.4 μM each primer, 0.2 μM probe, and 50 nM ROX reference dye in a Quantstudio 3 thermocycler using 40 cycles of two-step PCR with 95°C for lysis and 65°C for the annealing and extension temperature. Primers and probes were designed using Primer3plus using the primer length, melting temperature ranges, and other thermodynamic inputs (84, 85). These parameters are specified in the template file provided at https://doi.org/10.6084/m9.figshare.24328933. Three sets of primer pairs and probes were designed to amplify the ON state (flipping boundary), total copies of the reporter plasmid (plasmid ori), and E.coli chromosome (dcp gene) in a single triplex reaction, and absolute copies were obtained by fitting Cq values to a standard curve (Fig. S11). The fraction of ON state plasmid was obtained by dividing the copies of the ON state by the total plasmid. Details of the qPCR primer and probe sequences are available in Table S3.

### Analysis of memory stability

To test the temporal stability of the memory, *E. coli* MG1655 was transformed with the memory-reporter plasmid sets, and three independent colonies were picked and grown in M9-glucose with antibiotics (500  $\mu$ L) in deep-well blocks while shaking at 650 rpm at 37°C. Every 24 hours, the cultures were diluted ~1:500 into fresh media using 96-well replicator pins, and the process was repeated for 8 days. Arabinose or C12-AHL were included in the media only between day –1 and day 0, and cells were washed with PBS before subculturing. Aliquots of the cultures at the end of each day were diluted 1:100 in PBST and used for flow cytometry. The same cultures were also subjected to qPCR after heat lysis.

### **Statistics**

Data points presented represent three biological replicates derived from independent colonies with each replicate paired between exposure vs no exposure conditions and over the time course. *P*-values were obtained using one or two-tailed paired samples *t*-tests. In cases where week-long serial culturing was performed, we evaluated the significance of values observed on days days –1 or 1 and 8.

### **Software**

DNA sequences were stored, annotated, aligned, and assembled *in silico* using Benchling cloud software. Data analysis and plotting was performed in R software using ggplot2 and Rmarkdown. Automated R-based workflows were used for analysis of flow cytometry (https://dx.doi.org/10.6084/m9.figshare.23681499) and qPCR data (https://dx.doi.org/10.6084/m9.figshare.23681496). Illustrations were prepared in Inkscape.

### **ACKNOWLEDGMENTS**

We are grateful for the support from the National Science Foundation under grants 1805901 (to L.B.S. and J.J.S.), 2223678 (to L.B.S. and J.J.S.), and 2237052 (L.B.S.). This research was also supported by a Johnson & Johnson WiSTEM2D Award (L.B.S.) and the Gordon and Betty Moore Foundation (J.J.S.).

Additionally, we wish to acknowledge insightful discussions with Dr. Charilaos Giannitsis and plasmid design assistance from Dr. Shyam Bhakta.

### **AUTHOR AFFILIATIONS**

<sup>1</sup>Systems, Synthetic, and Physical Biology Graduate Program, Rice University, Houston, Texas, USA

<sup>2</sup>Department of BioSciences, Rice University, Houston, Texas, USA

<sup>5</sup>Department of Civil and Environmental Engineering, Rice University, Houston, Texas, USA

### **AUTHOR ORCIDs**

Prashant Bharadwaj Kalvapalle http://orcid.org/0000-0002-8255-3623

Jonathan J. Silberg http://orcid.org/0000-0001-5612-0667

Lauren B. Stadler http://orcid.org/0000-0001-7469-1981

### **FUNDING**

Funder	Grant(s)	Author(s)
National Science Foundation (NSF)	1805901, 2223678, 2237052	Prashant Bharadwaj Kalvapalle
		Swetha Sridhar
		Jonathan J. Silberg
		Lauren B. Stadler
Auris   Johnson and Johnson (J&J)	WiSTEM2D	Prashant Bharadwaj Kalvapalle
		Lauren B. Stadler
Gordon and Betty Moore Foundation (GBMF)		Jonathan J. Silberg

### **AUTHOR CONTRIBUTIONS**

Prashant Bharadwaj Kalvapalle, Conceptualization, Data curation, Formal analysis, Funding acquisition, Investigation, Methodology, Validation, Visualization, Writing – original draft, Writing – review and editing | Swetha Sridhar, Formal analysis, Visualization, Writing – review and editing | Jonathan J. Silberg, Conceptualization, Formal analysis, Funding acquisition, Investigation, Project administration, Resources, Supervision, Writing – original draft, Writing – review and editing.

### **DATA AVAILABILITY**

Data underlying the figures along with the processing R scripts are available upon request. The whole genome sequence data for the wastewater isolates, including raw fastq and assembled genomes, were deposited in NCBI (PRJNA1050252). GenBank files detailing the full plasmid sequences are available at https://doi.org/10.6084/m9.fig-share.25308625.

### **ADDITIONAL FILES**

The following material is available online.

### Supplemental Material

**Supplemental figures and tables (AEM02363-23-s0001.pdf).** Figures S1 to S11 and Tables S1 to S5.

<sup>&</sup>lt;sup>3</sup>Department of Bioengineering, Rice University, Houston, Texas, USA

<sup>&</sup>lt;sup>4</sup>Department of Chemical and Biomolecular Engineering, Rice University, Houston, Texas, USA

### **REFERENCES**

- Libis V, Delépine B, Faulon JL. 2016. Sensing new chemicals with bacterial transcription factors. Curr Opin Microbiol 33:105–112. https:// doi.org/10.1016/j.mib.2016.07.006
- Chang C, Stewart RC. 1998. The two-component system: regulation of diverse signaling pathways in prokaryotes and eukaryotes. Plant Physiol 117:723–731. https://doi.org/10.1104/pp.117.3.723
- Koretke KK, Lupas AN, Warren PV, Rosenberg M, Brown JR. 2000. Evolution of two-component signal transduction. Mol Biol Evol 17:1956–1970. https://doi.org/10.1093/oxfordjournals.molbev.a026297
- Del Valle I, Fulk EM, Kalvapalle P, Silberg JJ, Masiello CA, Stadler LB. 2021. Translating new synthetic biology advances for biosensing into the earth and environmental sciences. Front Microbiol 11:618373. https:// doi.org/10.3389/fmicb.2020.618373
- Bereza-Malcolm LT, Mann G, Franks AE. 2015. Environmental sensing of heavy metals through whole cell microbial biosensors: a synthetic biology approach. ACS Synth Biol 4:535–546. https://doi.org/10.1021/ sb500286r
- van der Meer JR, Belkin S. 2010. Where microbiology meets microengineering: design and applications of reporter bacteria. Nat Rev Microbiol 8:511–522. https://doi.org/10.1038/nrmicro2392
- Jung JK, Alam KK, Verosloff MS, Capdevila DA, Desmau M, Clauer PR, Lee JW, Nguyen PQ, Pastén PA, Matiasek SJ, Gaillard J-F, Giedroc DP, Collins JJ, Lucks JB. 2020. Cell-free biosensors for rapid detection of water contaminants. Nat Biotechnol 38:1451–1459. https://doi.org/10.1038/ s41587-020-0571-7
- DeAngelis KM, Ji P, Firestone MK, Lindow SE. 2005. Two novel bacterial biosensors for detection of nitrate availability in the rhizosphere. Appl Environ Microbiol 71:8537–8547. https://doi.org/10.1128/AEM.71.12. 8537-8547.2005
- DeAngelis KM, Lindow SE, Firestone MK. 2008. Bacterial quorum sensing and nitrogen cycling in rhizosphere soil. FEMS Microbiol Ecol 66:197– 207. https://doi.org/10.1111/j.1574-6941.2008.00550.x
- Shetty RS, Deo SK, Shah P, Sun Y, Rosen BP, Daunert S. 2003. Luminescence-based whole-cell-sensing systems for cadmium and lead using genetically engineered bacteria. Anal Bioanal Chem 376:11–17. https:// doi.org/10.1007/s00216-003-1862-9
- Koch B, Worm J, Jensen LE, Højberg O, Nybroe O. 2001. Carbon limitation induces σS-dependent gene expression in *Pseudomonas fluorescens* in soil. Appl Environ Microbiol 67:3363–3370. https://doi.org/ 10.1128/AEM.67.8.3363-3370.2001
- Pini F, East AK, Appia-Ayme C, Tomek J, Karunakaran R, Mendoza-Suárez M, Edwards A, Terpolilli JJ, Roworth J, Downie JA, Poole PS. 2017. Bacterial biosensors for in vivo spatiotemporal mapping of root secretion. Plant Physiol 174:1289–1306. https://doi.org/10.1104/pp.16. 01302
- Herron PM, Gage DJ, Arango Pinedo C, Haider ZK, Cardon ZG. 2013.
   Better to light a candle than curse the darkness: illuminating spatial localization and temporal dynamics of rapid microbial growth in the rhizosphere. Front Plant Sci 4:323. https://doi.org/10.3389/fpls.2013. 00323
- Herron PM, Gage DJ, Cardon ZG. 2010. Micro-scale water potential gradients visualized in soil around plant root tips using microbiosensors. Plant Cell Environ 33:199–210. https://doi.org/10.1111/j.1365-3040.2009. 02070.x
- Yeon K-M, Cheong W-S, Oh H-S, Lee W-N, Hwang B-K, Lee C-H, Beyenal H, Lewandowski Z. 2009. Quorum sensing: a new biofouling control paradigm in a membrane bioreactor for advanced wastewater treatment. Environ Sci Technol 43:380–385. https://doi.org/10.1021/ es8019275
- Paton GI, Reid BJ, Semple KT. 2009. Application of a luminescence-based biosensor for assessing naphthalene biodegradation in soils from a manufactured gas plant. Environ Pollut 157:1643–1648. https://doi.org/ 10.1016/j.envpol.2008.12.020
- Ma Z, Li Y, Lu Z, Pan J, Li M. 2023. A novel biosensor-based method for the detection of p-nitrophenol in agricultural soil. Chemosphere 313:137306. https://doi.org/10.1016/j.chemosphere.2022.137306
- Bringhurst RM, Cardon ZG, Gage DJ. 2001. Galactosides in the rhizosphere: utilization by Sinorhizobium meliloti and development of a

- biosensor. Proc Natl Acad Sci U S A 98:4540–4545. https://doi.org/10.1073/pnas.071375898
- Camilli A, Beattie DT, Mekalanos JJ. 1994. Use of genetic recombination as a reporter of gene expression. Proc Natl Acad Sci U S A 91:2634–2638. https://doi.org/10.1073/pnas.91.7.2634
- Gao M, Teplitski M. 2008. RIVET—A tool for in vivo analysis of symbiotically relevant gene expression in Sinorhizobium meliloti. Mol Plant Microbe Interact 21:162–170. https://doi.org/10.1094/MPMI-21-2-0162
- Perli SD, Cui CH, Lu TK. 2016. Continuous genetic recording with selftargeting CRISPR-Cas in human cells. Science 353:aag0511. https://doi. org/10.1126/science.aag0511
- Tang W, Liu DR. 2018. Rewritable multi-event analog recording in bacterial and mammalian cells. Science 360:eaap8992. https://doi.org/ 10.1126/science.aap8992
- Shipman SL, Nivala J, Macklis JD, Church GM. 2016. Molecular recordings by directed CRISPR spacer acquisition. Science 353:aaf1175. https://doi. org/10.1126/science.aaf1175
- Sheth RU, Yim SS, Wu FL, Wang HH. 2017. Multiplex recording of cellular events over time on CRISPR biological tape. Science 358:1457–1461. https://doi.org/10.1126/science.aao0958
- Schmidt F, Zimmermann J, Tanna T, Farouni R, Conway T, Macpherson AJ, Platt RJ. 2022. Noninvasive assessment of gut function using transcriptional recording sentinel cells. Science 376:eabm6038. https:// doi.org/10.1126/science.abm6038
- Zamft BM, Marblestone AH, Kording K, Schmidt D, Martin-Alarcon D, Tyo K, Boyden ES, Church G. 2012. Measuring cation dependent DNA polymerase fidelity landscapes by deep sequencing. PLos One 7:e43876. https://doi.org/10.1371/journal.pone.0043876
- Bhan NJ, Strutz J, Glaser J, Kalhor R, Boyden E, Church G, Kording K, Tyo KEJ. 2019. Recording temporal data onto DNA with minutes resolution. bioRxiv. https://doi.org/10.1101/634790
- Kalvapalle PB, Staubus A, Dysart MJ, Gambill L, Reyes Gamas K, Chieh Lu L, Silberg JJ, Stadler LB, Chappell J. 2023. Information storage across a microbial community using universal RNA memory. bioRxiv. https://doi. org/10.1101/2023.04.16.536800
- Sheth RU, Wang HH. 2018. DNA-based memory devices for recording cellular events. Nat Rev Genet 19:718–732. https://doi.org/10.1038/ s41576-018-0052-8
- Brown WRA, Lee NCO, Xu Z, Smith MCM. 2011. Serine recombinases as tools for genome engineering. Methods 53:372–379. https://doi.org/10. 1016/j.ymeth.2010.12.031
- Stark WM. 2017. Making serine integrases work for us. Curr Opin Microbiol 38:130–136. https://doi.org/10.1016/j.mib.2017.04.006
- 32. Thorpe HM, Smith MCM. 1998. *In vitro* site-specific integration of bacteriophage DNA catalyzed by a recombinase of the resolvase/invertase family. Proc Natl Acad Sci U S A 95:5505–5510. https://doi.org/10.1073/pnas.95.10.5505
- Lee SH, Butler SM, Camilli A. 2001. Selection for in vivo regulators of bacterial virulence. Proc Natl Acad Sci U S A 98:6889–6894. https://doi. org/10.1073/pnas.111581598
- Staib P, Kretschmar M, Nichterlein T, Köhler G, Michel S, Hof H, Hacker J, Morschhäuser J. 1999. Host-induced, stage-specific virulence gene activation in *Candida albicans* during infection. Mol Microbiol 32:533– 546. https://doi.org/10.1046/j.1365-2958.1999.01367.x
- Lowe AM, Beattie DT, Deresiewicz RL. 1998. Identification of novel staphylococcal virulence genes by in vivo expression technology. Mol Microbiol 27:967–976. https://doi.org/10.1046/j.1365-2958.1998.00741.x
- Casavant NC, Beattie GA, Phillips GJ, Halverson LJ. 2002. Site-specific recombination-based genetic system for reporting transient or low-level gene expression. Appl Environ Microbiol 68:3588–3596. https://doi.org/ 10.1128/AEM.68.7.3588-3596.2002
- 37. Casavant NC, Thompson D, Beattie GA, Phillips GJ, Halverson LJ. 2003. Use of a site-specific recombination-based biosensor for detecting bioavailable toluene and related compounds on roots. Environ Microbiol 5:238–249. https://doi.org/10.1046/j.1462-2920.2003.00420.x
- He L, Li Y, Li Y, Pu W, Huang X, Tian X, Wang Y, Zhang H, Liu Q, Zhang L, et al. 2017. Enhancing the precision of genetic lineage tracing using dual recombinases. Nat Med 23:1488–1498. https://doi.org/10.1038/nm.4437

- Zinyk DL, Mercer EH, Harris E, Anderson DJ, Joyner AL. 1998. Fate mapping of the mouse midbrain-hindbrain constriction using a sitespecific recombination system. Curr Biol 8:665–668. https://doi.org/10. 1016/s0960-9822(98)70255-6
- De Kievit TR, Gillis R, Marx S, Brown C, Iglewski BH. 2001. Quorumsensing genes in *Pseudomonas aeruginosa* biofilms: their role and expression patterns. Appl Environ Microbiol 67:1865–1873. https://doi. org/10.1128/AEM.67.4.1865-1873.2001
- Kirisits MJ, Parsek MR. 2006. Does *Pseudomonas aeruginosa* use intercellular signalling to build biofilm communities? Cell Microbiol 8:1841–1849. https://doi.org/10.1111/j.1462-5822.2006.00817.x
- Sahreen S, Mukhtar H, Imre K, Morar A, Herman V, Sharif S. 2022. Exploring the function of quorum sensing regulated biofilms in biological wastewater treatment: a review. Int J Mol Sci 23:9751. https://doi.org/10.3390/ijms23179751
- Johnsen AR, Karlson U. 2004. Evaluation of bacterial strategies to promote the bioavailability of polycyclic aromatic hydrocarbons. Appl Microbiol Biotechnol 63:452–459. https://doi.org/10.1007/s00253-003-1265-z
- Yang L, Nielsen AAK, Fernandez-Rodriguez J, McClune CJ, Laub MT, Lu TK, Voigt CA. 2014. Permanent genetic memory with >1-byte capacity. Nat Methods 11:1261–1266. https://doi.org/10.1038/nmeth.3147
- Salis HM, Mirsky EA, Voigt CA. 2009. Automated design of synthetic ribosome binding sites to control protein expression. Nat Biotechnol 27:946–950. https://doi.org/10.1038/nbt.1568
- Engler C, Kandzia R, Marillonnet S. 2008. A one pot, one step, precision cloning method with high throughput capability. PLoS One 3:e3647. https://doi.org/10.1371/journal.pone.0003647
- Jack BR, Leonard SP, Mishler DM, Renda BA, Leon D, Suárez GA, Barrick JE. 2015. Predicting the genetic stability of engineered DNA sequences with the EFM calculator. ACS Synth Biol 4:939–943. https://doi.org/10. 1021/acssynbio.5b00068
- Cheng HY, Masiello CA, Del Valle I, Gao X, Bennett GN, Silberg JJ. 2018. Ratiometric gas reporting: a nondisruptive approach to monitor gene expression in soils. ACS Synth Biol 7:903–911. https://doi.org/10.1021/ acssynbio.7b00405
- Espah Borujeni A, Channarasappa AS, Salis HM. 2014. Translation rate is controlled by coupled trade-offs between site accessibility, selective RNA unfolding and sliding at upstream standby sites. Nucleic Acids Res 42:2646–2659. https://doi.org/10.1093/nar/gkt1139
- Calles B, Goñi-Moreno Á, de Lorenzo V. 2019. Digitalizing heterologous gene expression in Gram-negative bacteria with a portable ON/OFF module. Mol Syst Biol 15:e8777. https://doi.org/10.15252/msb.20188777
- Kotula JW, Kerns SJ, Shaket LA, Siraj L, Collins JJ, Way JC, Silver PA. 2014. Programmable bacteria detect and record an environmental signal in the mammalian gut. Proc Natl Acad Sci U S A 111:4838–4843. https://doi. org/10.1073/pnas.1321321111
- Sridhar S, Ajo-Franklin CM, Masiello CA. 2022. A framework for the systematic selection of biosensor chassis for environmental synthetic biology. ACS Synth Biol 11:2909–2916. https://doi.org/10.1021/ acssynbio.2c00079
- Chan DTC, Baldwin GS, Bernstein HC. 2023. Revealing the hostdependent nature of an engineered genetic inverter in concordance with physiology. Biodes Res 5:0016. https://doi.org/10.34133/bdr.0016
- Nayfach S, Roux S, Seshadri R, Udwary D, Varghese N, Schulz F, Wu D, Paez-Espino D, Chen I-M, Huntemann M, et al. 2021. A genomic catalog of Earth's microbiomes. Nat Biotechnol 39:499–509. https://doi.org/10. 1038/s41587-020-0718-6
- Sato Y, Hori T, Koike H, Navarro RR, Ogata A, Habe H. 2019. Transcriptome analysis of activated sludge microbiomes reveals an unexpected role of minority nitrifiers in carbon metabolism. Commun Biol 2:179. https://doi.org/10.1038/s42003-019-0418-2
- Daims H, Taylor MW, Wagner M. 2006. Wastewater treatment: a model system for microbial ecology. Trends Biotechnol 24:483–489. https://doi. org/10.1016/j.tibtech.2006.09.002
- Tan CH, Koh KS, Xie C, Zhang J, Tan XH, Lee GP, Zhou Y, Ng WJ, Rice SA, Kjelleberg S. 2015. Community quorum sensing signalling and quenching: microbial granular biofilm assembly. NPJ Biofilms Microbiomes 1:15006. https://doi.org/10.1038/npjbiofilms.2015.6

- De Beer D, Schramm A, Santegoeds CM, Kuhl M. 1997. A nitrite microsensor for profiling environmental biofilms. Appl Environ Microbiol 63:973–977. https://doi.org/10.1128/aem.63.3.973-977.1997
- Mills G, Fones G. 2012. A review of in situ methods and sensors for monitoring the marine environment. Sens Rev 32:17–28. https://doi.org/ 10.1108/02602281211197116
- Gage DJ, Herron PM, Arango Pinedo C, Cardon ZG. 2008. Live reports from the soil grain - the promise and challenge of microbiosensors. Funct Ecol 22:983–989. https://doi.org/10.1111/j.1365-2435.2008.01464.
- Riedel K, Hentzer M, Geisenberger O, Huber B, Steidle A, Wu H, Høiby N, Givskov M, Molin S, Eberl L. 2001. N-Acylhomoserine-lactone-mediated communication between Pseudomonas aeruginosa and Burkholderia cepacia in mixed biofilms. Microbiology (Reading) 147:3249–3262. https://doi.org/10.1099/00221287-147-12-3249
- Liu Z, Stirling FR, Zhu J. 2007. Temporal quorum-sensing induction regulates Vibrio cholerae biofilm architecture. Infect Immun 75:122–126. https://doi.org/10.1128/IAI.01190-06
- Borchardt MA, Boehm AB, Salit M, Spencer SK, Wigginton KR, Noble RT. 2021. The environmental microbiology minimum information (EMMI) guidelines: QPCR and dPCR quality and reporting for environmental microbiology. Environ Sci Technol 55:10210–10223. https://doi.org/10. 1021/acs.est.1c01767
- Zhao F, Heidrich ES, Curtis TP, Dolfing J. 2020. Understanding the complexity of wastewater: the combined impacts of carbohydrates and sulphate on the performance of bioelectrochemical systems. Water Res 176:115737. https://doi.org/10.1016/j.watres.2020.115737
- Delgado Vela J, Bristow LA, Marchant HK, Love NG, Dick GJ. 2021. Sulfide alters microbial functional potential in a methane and nitrogen cycling biofilm reactor. Environ Microbiol 23:1481–1495. https://doi.org/10. 1111/1462-2920.15352
- Lee K, Lee S, Lee SH, Kim S-R, Oh H-S, Park P-K, Choo K-H, Kim Y-W, Lee J-K, Lee C-H. 2016. Fungal quorum quenching: a paradigm shift for energy savings in membrane bioreactor (MBR) for wastewater treatment. Environ Sci Technol 50:10914–10922. https://doi.org/10.1021/acs.est. 6b00313
- Bouayed N, Dietrich N, Lafforgue C, Lee CH, Guigui C. 2016. Processoriented review of bacterial quorum quenching for membrane biofouling mitigation in membrane bioreactors (MBRs). Membranes (Basel) 6:52. https://doi.org/10.3390/membranes6040052
- Lee S, Park S-K, Kwon H, Lee SH, Lee K, Nahm CH, Jo SJ, Oh H-S, Park P-K, Choo K-H, Lee C-H, Yi T. 2016. Crossing the border between laboratory and field: bacterial quorum quenching for anti-biofouling strategy in an MBR. Environ Sci Technol 50:1788–1795. https://doi.org/10.1021/acs.est. 5b04795
- Xu Z, Thomas L, Davies B, Chalmers R, Smith M, Brown W. 2013. Accuracy and efficiency define Bxb1 integrase as the best of fifteen candidate serine recombinases for the integration of DNA into the human genome. BMC Biotechnol 13:87. https://doi.org/10.1186/1472-6750-13-87
- Hirning A, Bhakta S. 2023. SOB and SOC. Bennett Lab Wiki Rice University.
   Available from: https://wiki.rice.edu/confluence/display/BIODESIGN/SOB+and+SOC. Retrieved 13 Mar 2024.
- Ferrières L, Hémery G, Nham T, Guérout A-M, Mazel D, Beloin C, Ghigo J-M. 2010. Silent mischief: bacteriophage Mu insertions contaminate products of *Escherichia coli* random mutagenesis performed using suicidal transposon delivery plasmids mobilized by broad-host-range RP4 conjugative machinery. J Bacteriol 192:6418–6427. https://doi.org/10.1128/JB.00621-10
- AndrewH, Bhakta S. 2018. Phosphate-buffered saline (PBS). Bennett Lab Wiki - Rice University. Available from: https://wiki.rice.edu/confluence/ pages/viewpage.action?pageld=24430853. Retrieved 13 Mar 2024.
- Blattner FR, Plunkett III G, Bloch CA, Perna NT, Burland V, Riley M, Collado-Vides J, Glasner JD, Rode CK, Mayhew GF, Gregor J, Davis NW, Kirkpatrick HA, Goeden MA, Rose DJ, Mau B, Shao Y. 1997. The complete genome sequence of *Escherichia coli* K-12. Science 277:1453–1462. https://doi.org/10.1126/science.277.5331.1453
- Zong D, Bhakta S. 2023. M9 medium. Bennett Lab Wiki Rice University.
   Available from: https://wiki.rice.edu/confluence/display/BIODESIGN/M9+Medium. Retrieved 13 Mar 2024.
- Miyada CG, Stoltzfus L, Wilcox G. 1984. Regulation of the araC gene of Escherichia coli: catabolite repression, autoregulation, and effect on

- araBAD expression. Proc Natl Acad Sci U S A 81:4120–4124. https://doi.org/10.1073/pnas.81.13.4120
- Masiello CA, Chen Y, Gao X, Liu S, Cheng H-Y, Bennett MR, Rudgers JA, Wagner DS, Zygourakis K, Silberg JJ. 2013. Biochar and microbial signaling: production conditions determine effects on microbial communication. Environ Sci Technol 47:11496–11503. https://doi.org/ 10.1021/es401458s
- Gibson DG, Young L, Chuang R-Y, Venter JC, Hutchison CA, Smith HO. 2009. Enzymatic assembly of DNA molecules up to several hundred kilobases. Nat Methods 6:343–345. https://doi.org/10.1038/nmeth.1318
- Ondov BD, Treangen TJ, Melsted P, Mallonee AB, Bergman NH, Koren S, Phillippy AM. 2016. Mash: fast genome and metagenome distance estimation using MinHash. Genome Biol 17:132. https://doi.org/10.1186/ s13059-016-0997-x
- Castillo-Hair SM, Sexton JT, Landry BP, Olson EJ, Igoshin OA, Tabor JJ. 2016. FlowCal: a user-friendly, open source software tool for automatically converting flow cytometry data from arbitrary to calibrated units. ACS Synth Biol 5:774–780. https://doi.org/10.1021/acssynbio.5b00284
- Finak G, Jiang M. 2023. flowWorkspace: infrastructure for representing and interacting with gated and ungated cytometry data sets. Bioconductor version: release (3.17). Available from: https://bioconductor.org/ packages/flowWorkspace/. Retrieved 19 Jun 2019.

- 81. Jiang M, Ramey J, Finak G, Gottardo R. 2023. openCyto: hierarchical gating pipeline for flow cytometry data. Bioconductor version: release (3.17). Available from: https://bioconductor.org/packages/openCyto/. Retrieved 19 Jun 2023.
- JiangM. 2023. ggcyto: visualize cytometry data with ggplot. Bioconductor version: release (3.17). Available from: https://bioconductor.org/packages/ggcyto/. Retrieved 19 Jun 2023.
- Soejima T, Xiao J-Z, Abe F. 2016. A novel mechanism for direct real-time polymerase chain reaction that does not require DNA isolation from prokaryotic cells. Sci Rep 6:28000. https://doi.org/10.1038/srep28000
- Untergasser A, Cutcutache I, Koressaar T, Ye J, Faircloth BC, Remm M, Rozen SG. 2012. Primer3—new capabilities and interfaces. Nucleic Acids Res 40:e115–e115. https://doi.org/10.1093/nar/gks596
- Koressaar T, Remm M. 2007. Enhancements and modifications of primer design program Primer3. Bioinformatics 23:1289–1291. https://doi.org/ 10.1093/bioinformatics/btm091